Postindustrial Jute Waste as a Support for Nano-carbon Nitride Photocatalyst: Influence of the Chemical Pretreatment

Milica V. Carević *, Tatjana D. Vulić, Zoran V. Šaponjić, Nadica D. Abazović *, Mirjana I. Čomor

Posted Date: 17 June 2024

doi: 10.20944/preprints202406.1125.v1

Keywords: carbon-nitride; textile dye; photocatalysis; jute; post-industrial waste

 doi:10.20944/preprints202406.1125.v1

Article

Postindustrial Jute Waste as a Support for Nano-carbon Nitride Photocatalyst: Influence of the Chemical Pretreatment

Milica V. Carević [1,*], Tatjana D. Vulić [1], Zoran V. Šaponjić [2], Nadica D. Abazović [1,*] and Mirjana I. Čomor [1]

[1] Vinča Institute of Nuclear Sciences, National Institute of the Republic of Serbia, University of Belgrade, Mike Petrovića Alasa 12-14, 11351, Vinča, Belgrade, Serbia; tanja030@vin.bg.ac.rs (T.V.); mirjanac@vin.bg.ac.rs (M.Č.)

[2] Institute of General and Physical Chemistry, Belgrade, Studentski Trg 12/V, 11158, Belgrade, Serbia; zsaponjic@iofh.bg.ac.rs

* Correspondence: milicab@vin.bg.ac.rs (M.C.); kiki@vin.bg.ac.rs (N.A.)

Abstract: Non-woven jute (NWJ) produced from the carpet industry waste was oxidized by H2O2 or alkali treated by NaOH and compared with water-washed samples. Changes in the structure of the NWJ, tracked by XRD, showing that both chemical treatments disrupt hydrogen bond networks between cellulose Iβ chains of the NWJ fibers. Thereafter, nano carbon nitride (nCN) was impregnated, using layer-by-layer technique, onto water washed jute sample (nCN-Jw), NaOH treated sample (nCN-Ja) and H2O2 treated sample (nCN-Jo). Analysis of the FTIR spectra of the impregnated samples, revealed that nCN anchors to the water washed NWJ surface through hemicellulose and secondary hydroxyl groups of the cellulose. In the case of chemically treated samples nCN is preferentially bonded to the hydroxymethyl groups of cellulose. The stability and reusability of nCN-J samples were assessed by tracking the photocatalytic degradation of Acid Orange 7 (AO7) dye under simulated solar light irradiation. Results from up to ten consecutive photocatalytic cycles demonstrated varying degrees of effectiveness across different samples. nCN-Jo and nCN-Ja samples exhibited declining effectiveness over cycles, attributed to bond instability between CN and jute. In contrast, the nCN-Jw sample consistently maintained high degradation rates over ten cycles, with a dye removal percentage constantly above 90%.

Keywords: carbon-nitride; textile dye; photocatalysis; jute; post-industrial waste

1. Introduction

In three Asian countries (India, Bangladesh, and China), home for roughly 40% of the world 's population, 3.4 million metric tons [1] of the jute are produced annually. Jute is conventionally employed in industries where mechanical stability is required since its fibers are robust, firm, and non-stretchy. Approximately 80% of produced jute fibers are traditionally utilized as packaging material, while more than 15% is used as carpet backing and yarn [2].

Jute fibers have complex chemical composition, with three main components: cellulose (up to 63%), hemicellulose (21-24%) and lignin (up to 12%), while the remaining part is divided between inorganic water solubles, waxes and fats [2]. Due to the similar carbohydrate origin and abundance of the hydroxyl groups, cellulose fibers (linked glucose units) and amorphous hemicellulose (a combination of C5 and C6 monosaccharide units) are easily coupled by hydrogen bonds [2]. Lignin, a complex polymeric structure built from guaiacyl, syringyl and 4-hydroxylphenyl propane units [3] hence rich in carbon-carbon bonds, is resistant to fragmentation and degradation [4–6] and is responsible for thermal resistance and rigidity of the jute cell fibers [6]. Usage of the jute is somewhat hindered because of these characteristics, i.e., it cannot be used, for example, for apparel production.

 doi:10.20944/preprints202406.1125.v1

There are numerous examples in the literature of how its chemical, and consequently, mechanical properties can be altered by alkali or oxidative treatment, commonly used in the textile industry. Specifically, the removal of hemicellulose by alkali treatment results in a less dense and hard interfibrillar area, which permits fibrils to reorganize along the direction of tensile strain [7] and increases relative cellulose share and flexibility of the fiber. Furthermore, alkali treated fibers have a greater capacity for sorption of moisture, a characteristic attributed to the increased availability of hydroxyl groups on cellulose fibers following hemicellulose removal. [6] Oxidative treatment, in addition to improving the whiteness of the fibers by removing their natural color, can also have two chemical effects [8]: oxidation of cellulose, which results in the cleavage of carbon-carbon bonds and the production of dialdehydes [9], and oxidative depolymerization of lignin through cleavage of C-C links [8–10]. Due to the abundance of the hydroxyl groups, jute fiber provides sufficient connection sites for oxide and nitride-based semiconductor photocatalysts through hydrogen bonding, and as such can be very attractive for the application in photocatalysis as a photocatalyst's carrier, bypassing the common problem in heterogeneous photocatalysis: photocatalysts retrieval from the reaction mixture and its reuse in the consecutive processes.

Jute based carpet waste, produced when a surplus of the weft yarns is trimmed off to provide equal carpet edges [11] can be transformed to nonwoven material by needle punch process. In our previous study [12] chemically untreated NWJ is utilized as a carrier of the carbon-nitride nanosheets (n-C_3N_4) and probed in photocatalytic degradation of three textile dyes. Fairly constant effectiveness in the three consecutive photocatalytic cycles proved the relatively strong and stable bonding between nCN and untreated jute-based textile waste.

To compare the effects of various chemical treatments on the semiconductor bonding on the surface of the fiber and, in turn, on the photocatalytic effectiveness of the fixed photocatalyst, this study treats NWJ produced from carpet industry waste through either an oxidative or an alkali treatment before applying nCN.

2. Materials and Methods

2.1. Materials

The following commercial chemicals were used: Urea (VWR, Belgium), Acid orange 7 (AO7, Color index - 15510, Cassela, Germany), Sodium hydroxide (Sigma Aldrich, Germany), Hydrogen peroxide (Chemsolute, The Geyer, Germani), Acetic acid (Sigma Aldrich, Switzerland). All chemicals were used as received. Non-woven jute was supplied by the company "Meteks", Serbia. In all experiments ultrapure water (4-6 x 10^{-8} Ω-1cm-1) from Milli Q water system was used.

2.2. Characterization

X-ray diffraction (XRD) patterns of all samples were collected using a Philips PW 1050 powder diffractometer (scanning technique: step size = 0.05, counting time = 5 s/step) with Ni filtered Cu Kα radiation (λ = 0.1542 nm). The average crystallite size D (nm) was determined from XRD patterns according to the Scherrer equation Eq. 1 [13]:

$$\boldsymbol{D = \frac{k\lambda}{\beta \cos\theta}} \quad (1)$$

where k is a constant equal to 0.94, λ is the wavelength of the X-rays equal to 0.1542 nm, β is the full-width at half-maximum of the X-ray diffraction peak at θ, the Bragg angle of the peak. The Z-value which indicates whether cellulose is Iα (Z>0) or Iβ (Z<0) was calculated from Eq. 2 [13]:

$$\boldsymbol{Z = 1693d1 - 902d2 - 549} \quad (2)$$

where d1 is the d-spacing of the Iβ (1-10) lattice plane and d2 is the d-spacing of the Iβ (110) lattice plane. The crystalline index (Cr.I.) was calculated using the empirical method proposed by Segal Eq. 3 [13]:

 doi:10.20944/preprints202406.1125.v1

$$Cr.I. = \frac{(I_{200} - I_{am})}{I_{200}} \, x \, 100 \qquad (3)$$

where I_{200} is the maximum intensity of the (200) diffraction and I_{am} is the intensity of the diffraction at 2θ~18°.

Surface morphologies and qualitative chemical compositions over the jute samples surfaces were analyzed using Scios 2 Dual Beam scanning electron microscope (SEM, Thermo Fisher Scientific) equipped with an energy-dispersive X-ray spectroscope (EDS) at 10 kV of acceleration voltage. The samples were sputter-coated with gold (Au) and placed on a sample holder using double-sided adhesive carbon tape. The UV-Vis absorbance spectra were recorded in the spectral range from 200 to 900 nm using a UV-2600i spectrophotometer (Shimadzu Corporation).

Fourier-transform infrared (FTIR) spectroscopy measurements were performed by using a Nicolet 380 FTIR spectrometer (Thermo Scientific) in the attenuated total reflection (ATR) mode (Smart Orbit™ ATR attachment). FTIR spectra were taken in the spectral range from 4000 to 525 cm^{-1}.

2.3. Sample Preparation

nCN: Nano carbon nitride (nCN) samples were synthesized according to the previous report [12]. Detailed procedure is given in SM.

nCN-J: NWJ was utilized as the photocatalyst carrier. It was manufactured through a needle punching process from carpet fringes comprised primarily of jute, with a small polyamide content, which were obtained as post-industrial waste from the carpet industry. As received non-woven jute was cut into pieces measuring approximately 3 cm x 3 cm. Prior to the photocatalyst immobilization, the jute samples underwent various pretreatments:

Ja - The jute sample was treated with 30 mL of 1% NaOH aqueous solution for 30 minutes at room temperature. Afterward, the sample was neutralized with 1% acetic acid and subsequently rinsed in distilled water (3 x 600 mL).

Jo - The jute sample was treated with 30 mL of 2% H_2O_2 aqueous solution for 30 minutes at room temperature. Following that, the sample was rinsed in distilled water (3 x 600 mL).

Jw - The jute sample was rinsed in distilled water (3 x 600 mL).

The jute samples masses were measured before and after drying at 80 °C for 20 hours, as well as before and after the treatments with NaOH, H_2O_2 and H_2O. The moisture contents and the weight losses which occur as a result of jute samples pretreatments were calculated using the direct gravimetric method. Results are shown in Table 1.

nCN-Ja, nCN-Jo and nCN-Jw: The nCN photocatalyst was immobilized onto the pretreated jute samples (Ja, Jo and Jw) as follows: 50 mg of nCN were dispersed in 25 mL of H_2O using ultrasonication for 30 minutes. The photocatalyst dispersion was drop coated layer-by-layer on jute sample in multistep process. In each step 3 mL of the photocatalyst dispersion were added drop-by-drop onto the surface of jute sample followed by drying at 80 °C before the next step. Finally, the jute samples were rinsed several times with deionized water and dried at 80 °C.

Table 1. Moisture content and weight loss NWJ samples.

Sample	Moisture content (%)	Weight loss (%)
Jw	7.6±0.3	1.3±0.1
Jo	7.6±0.3	3.5±0.4
Ja	7.6±0.2	5.1±0.4

2.4. Photocatalytic Activity Test

The photocatalytic performances of the nCN-J samples were investigated by monitoring the photodegradation of the textile dye AO7 (textile, acid, azo-dye; structural formula given in SM) under simulated solar light. All details regarding performed photocatalytic tests are given in SM. To

 doi:10.20944/preprints202406.1125.v1

determine the stability and reusability, the photocatalytic experiments were conducted in up to ten consecutive cycles. After each cycle, nCN-J sample was air dried at 80 °C and reused in the next cycle.

3. Results and Discussion

3.1. Characterization of the NWJ

As it is already noted, three main components of the jute fibers are cellulose, hemicellulose and lignin. While hemicellulose and lignin are amorphous, cellulose is semi-crystalline, and peaks present in the diffraction patterns of jute samples, (Figure 1), originate from the cellulose crystal planes. Cellulose is compiled of β-D-anhydroglucopyranose units (AGU) linked by β (1→4) ether bonds [14], forming chains, which are interconnected by hydrogen bonds, and their arrangement defines different polymorphs of the cellulose.

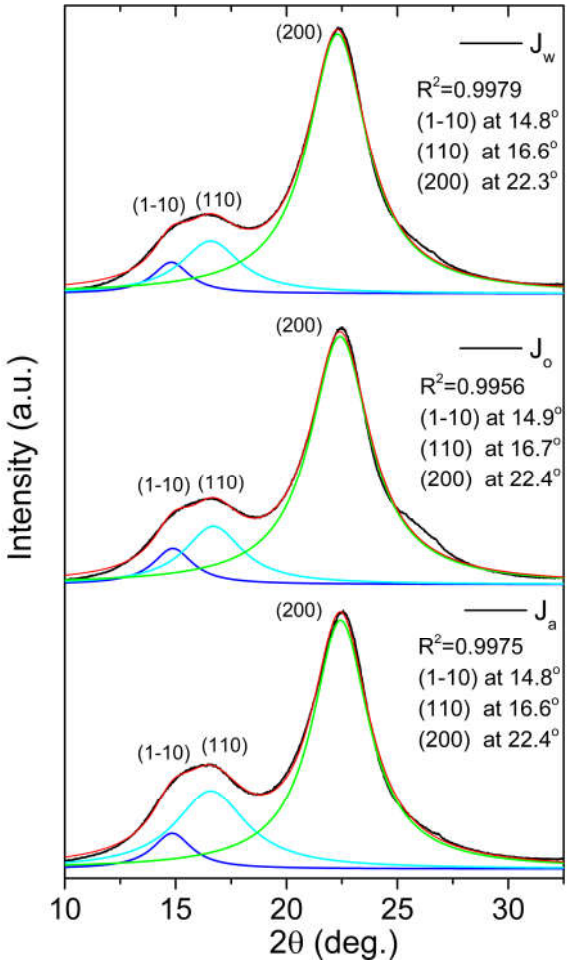

Figure 1. Deconvoluted XRD patterns of Jw (water-washed), Jo (treated with hydrogen-peroxide) and Ja (alkali-treated) jute samples.

Due to high share of the amorphous components, to accurately determine peak positions and intensities, d-spacings and crystallite sizes (D), obtained diffractograms were deconvoluted (Figures 1 and S1). Applying Eq. 2 on the obtained XRD patterns (Figure 1), Z values were calculated (Table 2) for all three NWJ samples, proving that predominant crystal polymorph of cellulose is Iβ, whose monoclinic unit cell is formed of two parallel cellulose chains interconnected by hydrogen bond network, with (1-10), (110) and (200) characteristic crystal planes (at 14.3-14.6°, at about 16.0°, and at 22.2-22.4°, respectively [13]) . Using Segal's eq. (Eq. 3) crystalline indexes, indicators of the share of the crystalline cellulose in the samples, are calculated for all three jute samples (Table 2). Changes in the crystalline index values can be induced by two major processes: a) The removal of non-cellulose

 doi:10.20944/preprints202406.1125.v1

components which leads to the reduction of the amorphous fraction in the sample, thereby increasing the relative share of the cellulose and consequently the crystalline index; b) destruction of the hydrogen bond network of crystalline cellulose, leading to increase of the amorphous cellulose share, and consequently lowering of the crystalline index value. [15–17]

Table 2. Parameters calculated from deconvoluted XRD patterns.

Sample	Z	Cr.I. (%)	d(1-10) (nm)	d(110) (nm)	d(200) (nm)	D(1-10) (nm)	D(110) (nm)	D(200) (nm)
Jw	-11	75.0	0.60	0.53	0.40	4.14	2.58	2.59
Jo	-11	72.9	0.60	0.53	0.40	3.86	2.64	2.56
Ja	-11	70.6	0.60	0.53	0.40	3.91	2.16	2.73

To understand observed decreasing trend in Jw>Jo>Ja order and the changes induced by alkali or oxidative treatment, defining the specific cellulose structure is of immense importance. Detailed analysis of Iβ cellulose polymorph is given first by Nishiyama et.al. [18] and explained further by Eyley and Thielemans [14]. According to them, surface of the nanocrystal is made up of cellulose chains directed along (200) preferential lattice plane, where molecules are interconnected by hydrogen bonds between O3…O5 and O2…O6 hydroxyl groups. However, adjacent chains on the surface are linked by weak C-H…O hydrogen bonds and van der Waals interactions [14] placed along (110) and (1-10) planes, resulting in such an arrangement that hydroxymethyl and secondary hydroxyl groups (Scheme 1) are directed outside of the crystal [14]. These exposed groups are susceptible to the reaction with H_2O_2 or NaOH, leading to the destruction of hydrogen bond network, and depolymerization of the cellulose [19], which consequently leads to decreasing of the crystallite sizes along (110) and/or (1-10) planes (Table 2) and lowering of the crystallinity index.

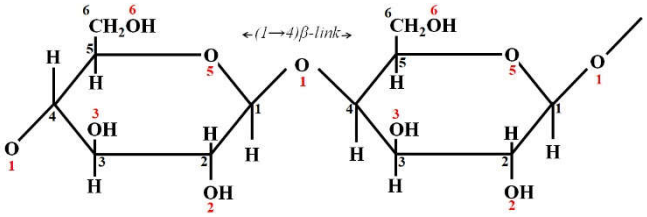

Scheme 1. Molecular structure of a cellulose unit.

The effect of the hydrogen peroxide is more pronounced along (1-10) lattice plane, while effect of NaOH is more expressed along (110) lattice plane. Increase of the crystallite size along the (200) lattice plane in the NaOH treated sample is the indication of cellulose chains reorientation along longitudinal direction, effect characteristic for alkali treated cellulose material [20]. However, disruption of the hydrogen bond network induced by applied mild oxidative or alkali treatment did not result in change of cellulose polymorph, as no shift towards lower angles characteristic for the cellulose II polymorph (at 12.1°(1-10), 20.1° (110) and 21.9° (020) [17]), are detected.

Influence of the chemical treatment on the amorphous components of the jute fibers is tracked by FTIR spectra (Figures 2 and S2). To compare intensities of the bands after chemical treatments, spectra are normalized. Band assignments are done according to literature data [21] and listed in Table 3.

 doi:10.20944/preprints202406.1125.v1

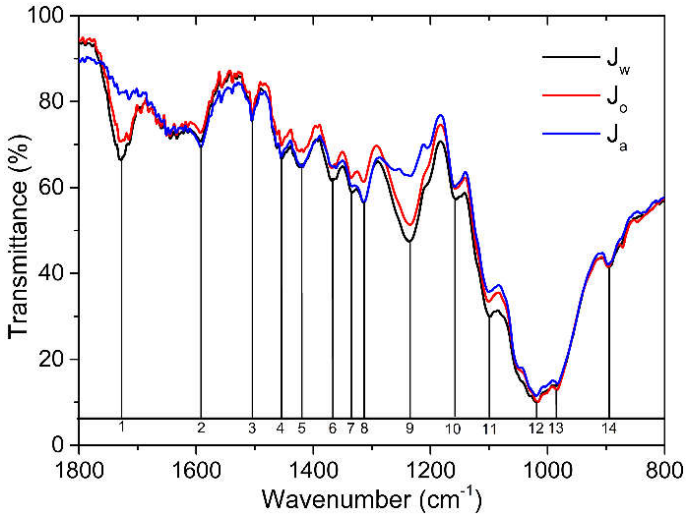

Figure 2. FTIR spectra of jute samples.

Although the main expected effect of treatment with hydrogen peroxide was removal of the lignin through its oxidative depolymerization and cleavage of C-C bonds [8–10], just slight decreases in the intensities of the bands related to aromatic skeletal vibration of lignin are observed, specifically bands centered at 1592 and 1506 cm^{-1}. Effect of hydrogen peroxide treatment is visible on all bands originating from O-H banding vibrations of cellulose and hemicellulose (bands at 1315, 1335, 1420 and 1456 cm^{-1}). This effect can be ascribed to the fact that H_2O_2 oxidizes secondary hydroxyl groups to ketone [22], which is in accordance with the results obtained from XRD findings: such a reaction would lead to the breaking of hydrogen bond networks in cellulose and lowering of the crystallinity index. Interestingly, hydroxymethyl groups of cellulose (C(6)…O(6)H) related bands centered at 1020 and 985 cm^{-1}, are not affected, although they could be oxidized to aldehyde or carboxylic acid upon reaction with hydrogen peroxide [22].

Table 3. FTIR spectra band assignment. HC-hemicellulose, L-lignin, C-cellulose.

	Wavenumber (cm^{-1})	Band assignment
1	1727	HC, C=O stretching in acetyl group and carboxylic group
2	1592	L, Aromatic skeletal vibration HC, (COO^- stretching)
3	1506	L, Aromatic skeletal vibration
4	1456	C, HC, O-H in-plane bending
5	1420	C, HC, O-H in-plane bending L, C-H bending in CH_3
6	1365	C, HC, C-H bending
7	1335	C, HC, O-H in-plane bending
8	1315	C, HC, O-H in-plane bending
9	1236	HC, C-O stretching in carboxylic acid
10	1155	C, HC, C-O-C antisymmetric stretching
11	1100	C, HC, C(2)…O(2)H stretching
12	1020	**C, C(6)…O(6)H stretching**
13	985	**C, C(6)…O(6)H stretching**
14	896	C, HC, antisymmetric vibration at the β-glycosidic linkage

Effect of the NaOH treatment is, on the other hand, easily observable: two strong bands placed at 1727 cm^{-1}, associated with C=O stretching vibration in acetyl group of hemicellulose and at 1236

 doi:10.20944/preprints202406.1125.v1

cm^{-1}, originating from C-O stretching vibration of carboxylic group of hemicellulose are almost completely disappeared confirming that alkali treatment of jute fibers even in low concentrations and relatively short times (3%, 30 min) leads to the dissolution of the amorphous hemicellulose. Again, bands related to hydroxymethyl groups of cellulose seem unaffected by alkali treatment.

SEM micrographs (Figure 3) of treated samples are compared to evaluate the impact of the chemical treatment on the fiber's surfaces. For the comparison, the SEM micrograph of the untreated, unwashed NWJ waste is also presented (Figure 3a). Untreated fabric is composed of fibers with a rough surface, covered with amorphous material and impurities. After simple washing with water (Figure 3b) major part of the impurities and water solubles are removed, resulting in fibers with relatively smooth surface, although amorphous components are still present. Similar cleaner surface of the fibers is characteristic for the jute sample treated with hydrogen peroxide (Figure 3c), but sporadically the formation of microcracks in the outer layer of the fibrils (indicated by arrows) is noticeable demonstrating that oxidative depolymerization of lignin probably started in minor extent. Finaly, alkali treated jute fibers (Figure 3d) suffered the biggest change as hemicellulose is moderately dissolved and removed (together with the impurities and other minor components), resulting in partially or completely separated microfibrils.

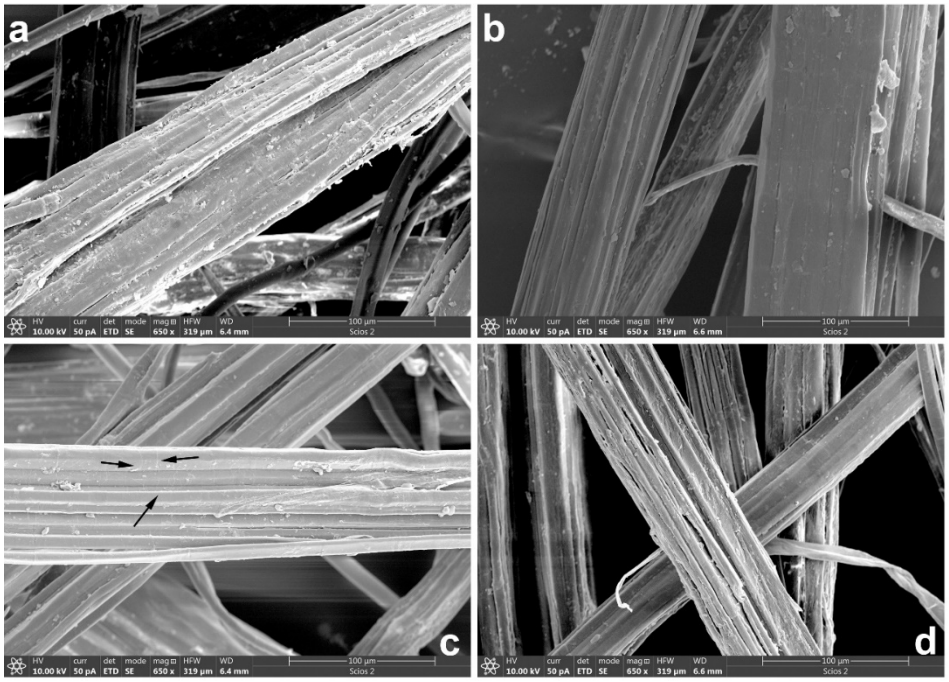

Figure 3. SEM images of jute samples: a) untreated, b) water-washed (Jw), c) treated with hydrogen peroxide (Jo) and d) alkali treated (Ja).

3.2. NWJ Impregnated with nCN

To clarify the mechanism of carbon nitride bonding to the jute surface, FTIR spectra of all three impregnated samples are compared with the spectra of unimpregnated counterparts (Figures 4 and S3). Upon impregnation, band at 1725 cm^{-1}, (C=O stretching vibration in acetyl group and carboxylic group of hemicellulose) of nCN-Jw sample is completely suppressed, indicating that this group is the one of carbon nitride anchoring points to the Jw sample surface (Figure 4).

 doi:10.20944/preprints202406.1125.v1

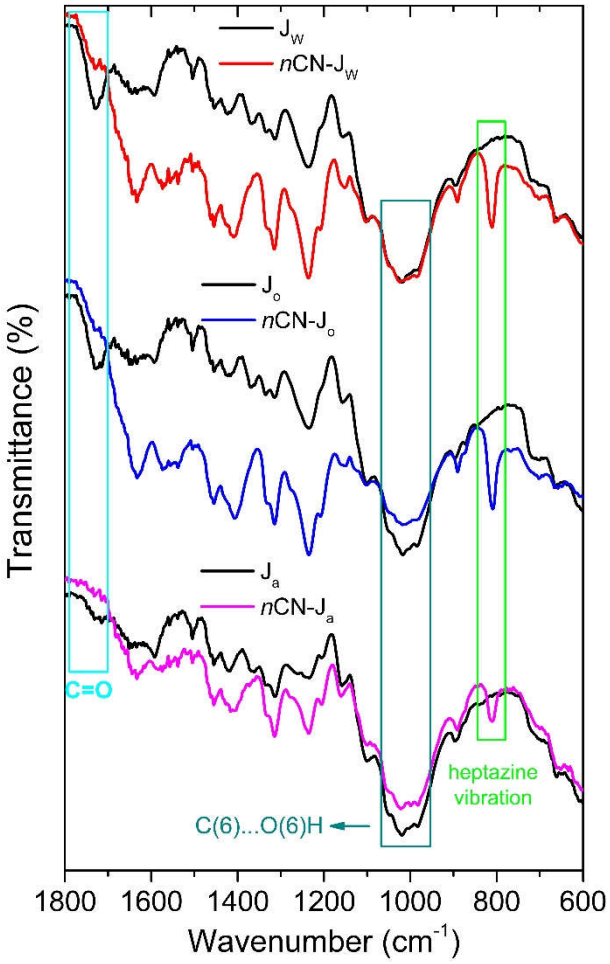

Figure 4. Comparative FTIR spectra of treated (black line) and nCN impregnated (colored line) jute samples.

The same band is repressed in the FTIR spectrum of the nCN-Jo sample (Figure 4b), but there is also significant reducing in the intensity of the bands related to (C(6)…O(6)H) vibrations of the hydroxymethyl groups of cellulose (centered at 1020 and 985 cm^{-1}). The same band intensity reduction is characteristic of the FTIR spectrum of nCN-Ja sample, where also the overall intensity of the nCN related bands is much lower compared to the other two jute samples, quite expected if the acetyl and/or carboxylic groups of hemicellulose (partially removed upon alkali treatment in the Ja sample) are the one of the points of the carbon nitride bonding.

The entire region between 1700 and 1100 cm^{-1} is hidden by carbon nitride bands, preventing detailed analysis of the possible interaction between amino groups of carbon nitride and OH groups of jute samples. However, some conditional conclusions can be drawn: both, oxidative and alkali treatment "neutralize" secondary hydroxyl groups of cellulose (first by oxidizing them to ketone [22], and the later by ionization to alkoxide [19]), hydrogen bond network of the cellulose is disrupted in both chemically treated samples, Jo and Ja, leaving hydroxymethyl group of the cellulose available for the interaction with the carbon nitride. These groups could be the main anchoring spots of the carbon nitride on the chemically treated jute surface. However, the same is not valid for the water washed sample: impregnation has no effect on the hydroxymethyl related band, probably because all secondary hydroxyl groups of cellulose were available for carbon nitride bonding, as well as hemicellulose.

Such differences in surface chemistry of the jute fibers, resulted in different carbon nitride distribution along the fiber upon impregnation (Figure 5).

 doi:10.20944/preprints202406.1125.v1

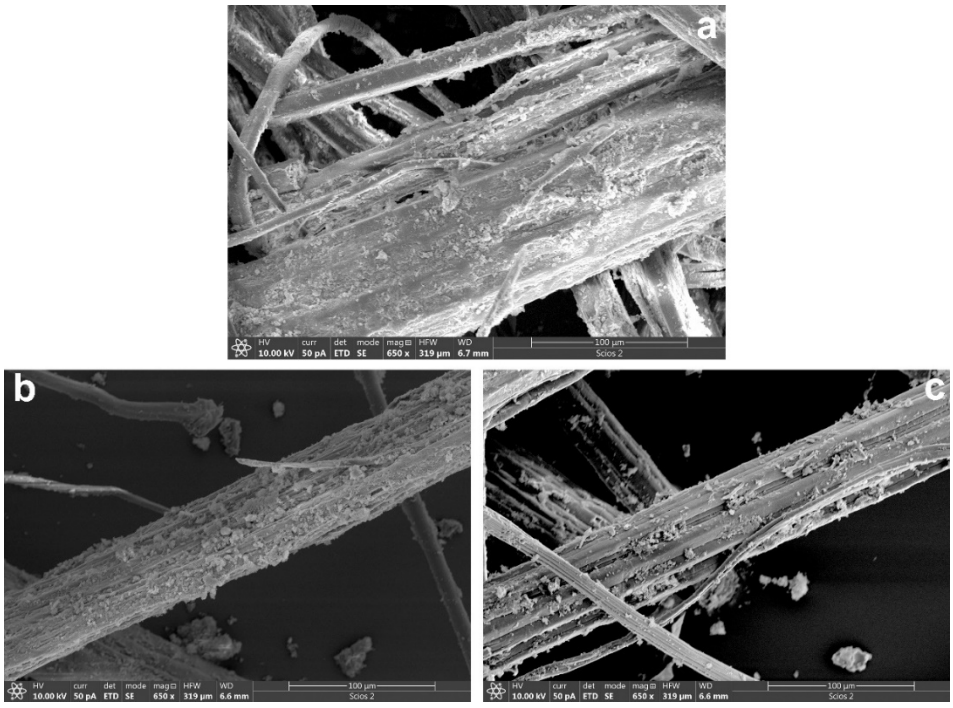

Figure 5. SEM images of impregnated jute samples: a) nCN-Jw, b) nCN-Jo and c) nCN-Ja.

SEM images (Figures 5a and 5b) of nCN-Jw and nCN-Jo samples underlined the importance of the hemicellulose presence, as carbon nitride is almost evenly distributed along the jute fibers, while for the alkali treated sample nCN-Ja (Figure 5c) chunks of carbon-nitride agglomerates are sporadically scattered on the jute fibers.

3.3. Photocatalytical Measurements

Finally, to evaluate stability of carbon nitride-jute bonding and reusability of NWJ in multiple consecutive photocatalytic cycles, impregnated samples were probed in photocatalytic degradation of the textile dye, AO7, under simulated solar light irradiation. Obtained results are presented in Figure 6, after 1h of irradiation, without adsorption of the dye that can occur during the system standing in the dark for the initial adsorption/desorption equilibration step (cumulative results presented in Figure S4).

Photocatalytic degradation of the AO7 on the nCN-Jw sample is constantly high through ten consecutive photocatalytic cycles, indicating the quality and stability of the carbon-nitride – jute bonding, i.e., almost no carbon nitride is lost through repeated cycles, keeping efficacy of dye removal above 90%. Exception is the ninth cycle with 82%, drop that can be explained by cumulative contamination of the carbon-nitride surface with the intermediates of the photocatalytic reaction.

Similar behavior is expressed by nCN-Jo sample. After the first sluggish cycle, in the next six cycles the percentage of the removed dye is above 90%. However, the last three cycles experienced a sharp decline in effectiveness reaching just 62% in the tenth cycle. Finally, after outstanding 94% of the dye removed in the first cycle, in the next four cycles effectiveness of the nCN-Ja sample suffered constant sharp decline, reaching only 40% in the final fifth cycle. Keeping in mind the poor distribution of the carbon nitride on the alkali treated fiber (Figure 5c), such a result is not surprising. However, another point regarding instability of carbon – nitride-jute bonding in chemically treated samples also must be considered: nCN is not a selective photocatalyst, meaning that photogenerated charges formed upon its illumination form radicals (mechanism explained in detail in [11]) which in turn non-selectively can react with all present species, not just AO7, including the carbon nitride-jute bond. Decline in the photocatalytic effectiveness of nCN-Jo and nCN-Ja samples can be a consequence of the breakage of the of the bond formed between amino group of the carbon nitride and

Preprints.org (www.preprints.org) | NOT PEER-REVIEWED | Posted: 17 June 2024 doi:10.20944/preprints202406.1125.v1

hydroxymethyl group of the cellulose, characteristic for both samples as confirmed by FTIR spectra. Such a hypothesis is further supported by the constantly high photocatalytic effectiveness of the nCN-Jw sample, for which it is expected that carbon-nitride is bonded to fiber's surface through hydrogen bond with secondary OH groups of cellulose and hemicellulose.

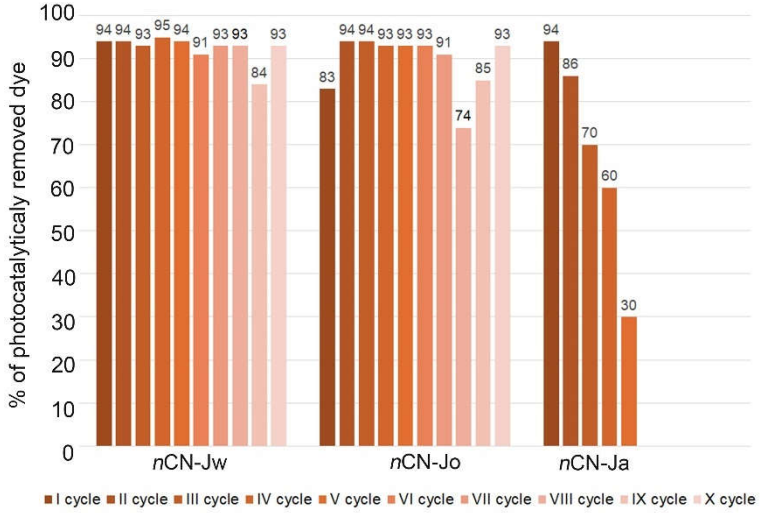

Figure 6. Percentage of photocatalyticaly removed dye using impregnated jute samples.

Additionally, FTIR spectra of the impregnated samples recorded after final photocatalytic experiments (Figures 7 and S5) revealed that:

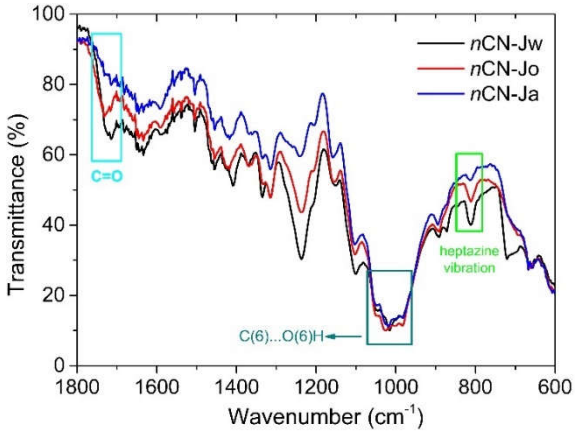

Figure 7. FTIR spectra of nCN-J samples after ten (nCN-Jw and nCN-Jo) or five (nCN-Ja) photocatalytic cycles.

- The band at ~1725cm^{-1} is recovered in the nCN-Jw and nCN-Jo samples, pointing to the breakage of the carbon-nitride-hemicellulose bond.
- Intensities of the bands related to hydroxymethyl group vibrations (at 1020 and 985 cm^{-1}) are fully recovered in the FTIR spectra of the nCN-Jo and nCN-Ja samples, indicating the detachment of the carbon-nitride from the cellulose.
- In all three spectra band at ~ 815 cm^{-1} (characteristic vibration of the heptazine) is present, proving presence of the carbon nitride in the impregnated samples, even after multiple photocatalytic cycles, but with significant differences in the intensities, which can be correlated to the lowering of the photocatalytic effectiveness stability in Jw>Jo>Ja order.

4. Conclusions

Jute post-industrial waste is pre-treated with hydrogen peroxide and NaOH, and then compared with the water-washed sample. Results from the XRD analysis indicated the profound effect that chemical treatment has on the cellulose fibers as both chemical treatments lead to the destruction of

 doi:10.20944/preprints202406.1125.v1

the hydrogen bond network between cellulose chains: oxidative treatment is mainly expressed along (1-10) lattice plane, while alkali treatment is more pronounced along (110) lattice plane of the cellulose. Therefore, mechanism of the carbon-nitride bonding to the jute fiber surface changes significantly: while in the water-washed sample major presumed anchoring points are secondary hydroxyl groups of the cellulose, in the chemically treated samples these are hydroxymethyl groups of the cellulose, as confirmed by FTIR spectra. SEM images revealed the differences in the fiber surface chemistry and the bonding mechanism, carbon nitride is the worst distributed over NaOH treated sample. Photocatalytic efficiency and stability of the impregnated samples drops in the Jw>Jo>Ja order.

Results obtained in this study can serve as a guideline for the studies related to the usage of any cellulose-based material as a photocatalyst's support and underline the importance of the thoughtful understanding of the chemical and structural processes implied upon chemical treatment of the textile fibers.

Finally, it has been demonstrated that jute waste, solely subjected to water washing to eliminate impurities and water-soluble compounds, exhibits notable potential as a support for nCN photocatalysts. The CN-Jw sample shows continuously high degradation rates over ten cycles, with minimal loss of carbon nitride and a dye removal percentage consistently above 90%.

Supplementary Materials: The following supporting information can be downloaded at Preprints.org, Table S1: Properties of the Acid Orange 7; Figures S1: XRD patterns of the NWJ samples: Jw (water-washed), Jo (treated with hydrogen peroxide) and Ja (alkali-treated); Figure S2. FTIR spectra of the NWJ samples; Figure S3. Comparative FTIR spectra of treated (black line) and nCN impregnated (colored line) jute samples; Figure S4. Percentage of the removed dye using nCN-J samples; Figure S5. FTIR spectra of nCN-J samples after ten (nCN-Jw and nCN-Jo) or five (nCN-Ja) photocatalytic cycles.

Author Contributions: Conceptualization, Investigation, Writing – Review & Editing M.V.C.; Investigation, Writing – Review & Editing T.D.V.; Writing – Review & Editing Z.V.Š.; Conceptualization, Supervision, Investigation, Writing – Original Draft N.D.A.; Conceptualization, Supervision, Writing – Review & Editing M.I.Č. All authors have read and agreed to the published version of the manuscript.

Funding: This research was funded by Science Fund of the Republic of Serbia, GRANT No.7673808.

Data Availability Statement: The original contributions presented in the study are included in the article/supplementary material, further inquiries can be directed to the corresponding author/s.

Acknowledgments: This research was supported by the Science Fund of the Republic of Serbia, GRANT No.7673808, Sustainable implementation of textile waste in treatment of polluted water-SORBTEX. The authors are grateful to Dr. Tanja Barudžija Vinča Institute of Nuclear Sciences, Nacional Institute of Republic of Serbia, Belgrade, Serbia, for XRD measurements and Dr. Jelena Potočnik, Vinča Institute of Nuclear Sciences, Nacional Institute of Republic of Serbia, Belgrade, Serbia, for SEM measurements.

Conflicts of Interest: The authors declare no conflicts of interest. The funders had no role in the design of the study; in the collection, analyses, or interpretation of data; in the writing of the manuscript; or in the decision to publish the results.

References

1. https://businessesranker.com/largest-producer-of-jute-in-the-world/1489/
2. Krishnan K.B.; Doraiswamy I.; Chellamani K.P. (2005) Jute. In:Franck RR (ed) Bast and other plant fibers, 1st edn.Woodhead Publishing Limited and CRC Press LCR,Cambridge, pp 24–94
3. Derkacheva O.; Sukhov D. Investigation of Lignins by FTIR Spectroscopy, *Macromol. Symp.* **2008**, *265*, 61–68. DOI:10.1002/masy.200850507
4. Kostic M.; Pejic B.; Skundric P. Quality of chemically modified hemp fibers, *Bioresour. Technol.* **2008**, *99*, 94–99. DOI: 10.1016/j.biortech.2006.11.050
5. Pejic B.M.; Kostic M.M.; Skundric P.D.; Praskalo J.Z. The effects of hemicelluloses and lignin removal on water uptake behavior of hemp fibers. *Bioresour. Technol.* **2008**, *99*, 7152–7159. DOI: 10.1016/j.biortech.2007.12.073

6. Ivanovska A.; Cerovic D.; Maletic S.; Jankovic Castvan I.; Asanovic K.; Kostic M. Influence of the alkali treatment on the sorption and dielectric properties of woven jute fabric, *Cellulose* **2019**, *26*, 5133-5146. DOI: 10.1007/s10570-019-02421-0
7. Gassan J.; Bledzki A.K. Alkali Treatment of Jute Fibers: Relationship Between Structure and Mechanical Properties, *Appl. Polym. Sci.* **1999**, *711*, p.623-629. DOI: 10.1002/(SICI)1097-4628(19990124)71:4<623::AID-APP14>3.0.CO;2-K
8. Lazic B.D.; Janjic S.D.; Korica M.; Pejic B.M.; Djokic V.R.; Kostic M.M. Electrokinetic and sorption properties of hydrogen peroxide treated flax fibers (*Linum usitatissimum L.*), *Cellulose* **2021**, *28*, 2889-2903. DOI: 10.1007/s10570-021-03686-0
9. López Durán V.; Larsson P.A.; Wågberg L. Chemical modification of cellulose-rich fibres to clarify the influence of the chemical structure on the physical and mechanical properties of cellulose fibres and thereof made sheets. *Carbohydr. Polym.* **2018**, *182*, 1-7. DOI: 10.1016/j.carbpol.2017.11.006.
10. Schutyser W.; Renders T.; Van den Bosch S.; Koelewijn S.F.; Beckham G.T.; Sels B.F. Chemicals from lignin: an interplay of lignocellulose fractionation, depolymerisation and upgrading. *Chem. Soc. Rev.* **2018**, *47(3)*, 852–908. DOI: 10.1039/C7CS00566K.
11. Kumar J.; Kumar K.; Kumar K.; Jaiswal B.; Verma R.K. Development of waste carpet (jute) and Multi-wall carbon nanotube incorporated epoxy composites for lightweight applications, *Progress in Rubber Plastics and Recycling Technology* **2022**, *38(3)*, 247–263. DOI: 10.1177/14777606221110252.
12. Carević M.V.; Vulić T.D.;, Šaponjić Z.V.; Mojović Z.D.; Abazović N.D.; Čomor M.I. Carbon nitride impregnated non-woven jute post-industrial waste in photocatalytic degradation of textile dyes, *Cellulose* **2024**, *31*, 5297-5312. DOI:10.1007/s10570-024-05908-7.
13. Poletto M.; Pistor V.; Zattera A.J. Structural Characteristics and Thermal Properties of Native Cellulose, DOI: 10.5772/50452, Chapter 2 in Cellulose - Fundamental Aspects, Edited by Theo van de Ven and Louis Godbout, IntechOpen, Rijeka, Croatia
14. Eyley S.; Thielemans W. Surface modification of cellulose nanocrystals, *Nanoscale* **2014**, *6*, 7764–7779. DOI: 10.1039/C4NR01756K.
15. Wang W.; Cai Z.; Yu J.;, Xia Z. Changes in Composition, Structure, and Properties of Jute Fibers after Chemical Treatments, *Fibers. Polym.* **2009**,*10(6)*, 776-780. DOI: 10.1007/s12221-009-0776-3.
16. Loganathan T.M.; Sultan M.T.H.; Ahsan Q.; Jawaid M.; Naveen J.; Shah A.U.M.; Hua L.S.; Characterization of alkali treated new cellulosic fibre from *Cyrtostachys renda*, *J. Mater. Res. Tech.* **2020**, *9(3)*, 3537-3546. DOI: 10.1016/j.jmrt.2020.01.091.
17. Ivanovska A.; Cerovic D.; Tadic N.; Jankovic Castvan I.; Asanovic K.; Kostic M. Sorption and dielectric properties of jute woven fabrics: Effect of chemical composition, *Ind. Crops. Prod.* **2019**,*140*, 111632. DOI: 10.1016/j.indcrop.2019.111632.
18. Nishiyama Y.; Langan P.; Chanzy H. Crystal Structure and Hydrogen-Bonding System in Cellulose Iβ from Synchrotron X-ray and Neutron Fiber Diffraction, *J. Am. Chem. Soc.* **2002**, *124*, 9074–9082. DOI: 10.1021/ja0257319.
19. Khan M.A.; Guru S.; Padmakaran P.; Mishra D.; Mudgal M.; Dhakad S. Characterisation Studies and Impact of Chemical Treatment on Mechanical Properties of Sisal Fiber, *Composite Interfaces* **2011**, *18*, 527-541. DOI: 10.1163/156855411X610250.
20. Lakshmanan A.; Ghosh R.K.; Dasgupta S.; Chakraborty S.; Ganguly P.K. Optimization of alkali treatment condition on jute fabric for the development of rigid biocomposite, *J. Ind. Text.* **2018**, *47*, 640-655. DOI: 10.1177/1528083716667259.
21. Horikawa Y.; Hirano S.; Mihashi A.; Kobayashi Y.; Zhai S.; Sugiyama J. Prediction of Lignin Contents from Infrared Spectroscopy: Chemical Digestion and Lignin/Biomass Ratios of *Cryptomeria japonica*, *Appl. Biochem. Biotechnol*. **2019**, *188(4)*, 1066-1076. DOI: 10.1007/s12010-019-02965-8.
22. Hellström P.; Heijnesson-Hultén A.; Paulsson M.; Håkansson H.; Germgård U. The effect of Fenton chemistry on the properties of microfibrillated cellulose, *Cellulose* **2014,** *21*, 1489–1503. DOI: 10.1007/s10570-014-0243-1.